

Quantification of the Acoustic Emissions of an Electric Ducted Fan Unit

Stefan Schoder¹, Jakob Schmidt², Andreas Furlinger³ and Manfred Kaltenbacher¹

¹TU Graz, IGTE, Graz, Austria, 8010

²TU Wien, Wien, Austria, 1040

³VOLARE GmbH, Mödling, Austria, 2340

stefan.schoder@tugraz.at

Abstract

Multiple aircraft manufacturers are developing novel electric aircraft concepts to explore the capabilities of modern electromobility. Their respective electric propulsion systems obtain different turbomachinery properties and exhibit different acoustical behavior than conventional combustion turbines. In collaboration with VOLARE GmbH, acoustic measurements were performed on subsonic electric ducted fans (EDF). The work examined the total sound power emissions and microphone array measurements to understand the dominant acoustic emissions and their respective prevailing source mechanisms. Measurements at discrete operating points and transient measurements across the total operating range were conducted to provide complete information on the EDF's acoustic behavior. The rotor-self noise and the rotor-stator interaction were identified as primary tonal sound sources, along with the highest broadband noise sources also being located on the rotor.

Additionally, far-field measurements of the unit's electric powertrain without load were conducted, which showed significant noise emissions from the periodic electromagnetic forces. An unexpected dependence on the rotational speed was detected in the powertrain's noise spectrum, contributing to the EDF's perceived acoustics. After processing the insights gained from the measuring campaign, a secondary noise reduction measure was designed.

1 Introduction

Electric propulsion has become a vital part of the aviation sector amongst electrically powered vertical take-off and land (eVTOL) aircraft. The primary acoustic sources of those eVTOL aircraft are their propulsion units, especially during vertical flight operation, where the propulsion units' thrust generates lift forces [1, 2]. One type of electric propulsion system is an EDF conceived as a single-stage axial fan, as shown in Figure 1, with its respective aerodynamic and electric components. We investigate acoustically the electric powertrain, consisting of an electronically commutated motor (ECM) and the respective motor controller. The measuring object considered

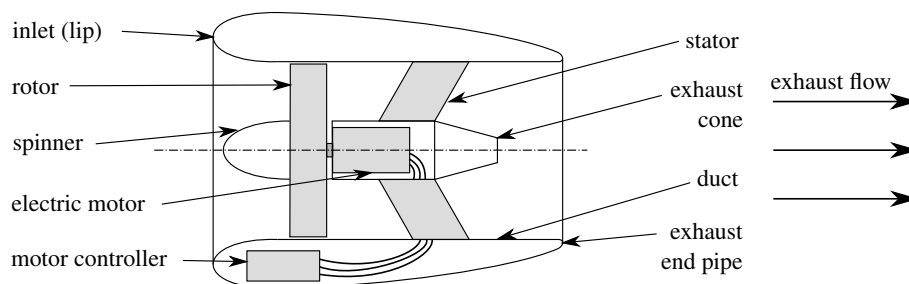


Figure 1: Visualisation of components in an operational single-stage axial-flow EDF system, adapted from [3].

for the subsequent examination is a subsonic, subscale, single-stage, axial-flow EDF unit. This EDF unit generates

Table 1: Aeroacoustic sources and characteristics in axial fans associated with the rotor, adapted from [12, 3].

	mechanism	tonal	narrowband	broadband
rotor self-noise	blade thickness noise	■		
	Gutin noise	■		
	boundary layer noise			■
	boundary layer separation noise	■		■
	trailing edge noise (laminar BL)	■		
	trailing edge noise (turbulent BL)	■		■
	blunt TE vortex shedding	■		
	tip noise			■
	turbulence ingestion (leading edge) noise			■
	unsteady loading noise	■		
	subharmonic tip noise		■	
	rotating stall		■	
	multiple pure tones	■		

aeroacoustic sound sources that are characteristic for axial fans and summarized in Table 1. Following former research, the primary acoustic sources of axial fans are aerodynamic [4]. Rotor-self noise, as well as noise due to rotor-stator flow wake interaction, excites sound pressure levels (SPL) at the blade passing frequency (BPF) [5, 6]

$$f_{\text{BPF}} = BN, \quad (1)$$

and its harmonic frequencies $f_{\text{BPF}n} = n f_{\text{BPF}}$, with B being the number of rotor blades, N the rotational speed, and n the harmonic multiplicity. Due to the decay of the acoustic field excited by subsonic rotor-self mechanisms inside circular ducts [5], the primary source mechanism at the BPF and its harmonics is expected to originate from the rotor-stator interactions. The fan's sound emissions are subject to the following investigation at different operating points. The acoustic characteristics of the measuring object during its operation were measured experimentally by total sound power measurements.

Another relevant sound source of EDFs, in particular, is the electric powertrain with a focus on the electric motor. Table 2 shows a summary of the possible source and attenuation mechanisms related to the electric motor placement inside the duct. The individual mechanisms are classified into tonal and broadband representation inside a measured spectrum. Furthermore, the excitation is classified as aeroacoustic, structural related, and electrodynamic. In addition, the electric drive parts, electronically commutated motor (ECM) and electronic speed controller (ESC), responsible for the acoustic emission, are provided. The noise emissions of an electronically

Table 2: Acoustic sources and characteristics in axial fans associated with the electric powertrain [3].

	mechanism	ECM	ESC	tonal	broadband
aeroac.	boundary layer noise	■	■		■
	vortex shedding	■	■	■	
	cavity resonance	■	■	■	
struct.	bearing noise	■		■	■
	ECM rotor unbalance	■		■	
	structural modes	■		■	
electrodyn.	tangential Lorentz force	■		■	
	normal Lorentz force	■		■	
	cogging torque	■		■	
	torque ripple	■		■	
	switching frequency		■	■	

commutated motor result from electromagnetic force and torque ripples during service and occur at different frequencies [7, 8, 9, 10]. The base frequency of the local forces

$$f_{\text{LF}} = 2pN, \quad (2)$$

and its harmonic frequencies $f_{\text{LF}n} = 2npN$, can be computed using the number of motor pole pairs p [7, 9, 10]. Based on these noise production and location of the energy conversion into acoustics, Figure 2 shows possible

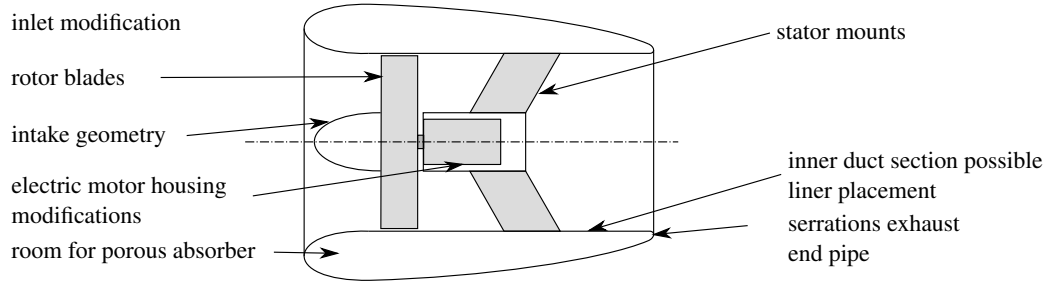


Figure 2: Visualisation of potential steering wheels for noise reduction at an EDF unit.

locations to apply noise mitigation measures. In the first study, acoustic liners partly cover the inner duct side. The back volume of the liners was treated according to the experience given in [13]. The underlying research was performed and published partly in [3].

2 Methodology

The EDF unit is examined acoustically at four operating points, which are defined in Table 3 with the rotational speed by a reference frequency f_{ref} . The subsonic behavior of the observed EDF unit is evident when looking at the

Table 3: Operating conditions of the measuring object at different operating points with N being described in dependence of the reference frequency f_{ref} .

operating point	N	M_{tip}	f_{BPF}	f_{LF}
OP 1	f_{ref}	0.18	700 Hz	1400 Hz
OP 2	$\frac{4}{3}f_{\text{ref}}$	0.24	933 Hz	1866 Hz
OP 3	$\frac{5}{3}f_{\text{ref}}$	0.30	1167 Hz	2343 Hz
OP 4	$2f_{\text{ref}}$	0.36	1400 Hz	2800 Hz

rotor blades' tip Mach number M_{tip} . The manufactured EDF unit number of electric motor pole pairs equals the rotor blades $p = B$. As a consequence, the frequency of the local electromagnetic forces coincides twice the BPF $f_{\text{LF}} = 2f_{\text{BPF}}$ of the EDF unit. Changing this attribute can reduce the emitted sound regarding the overall sound level. The sound power measurements were performed in a low-reflection measuring room with reflecting floor

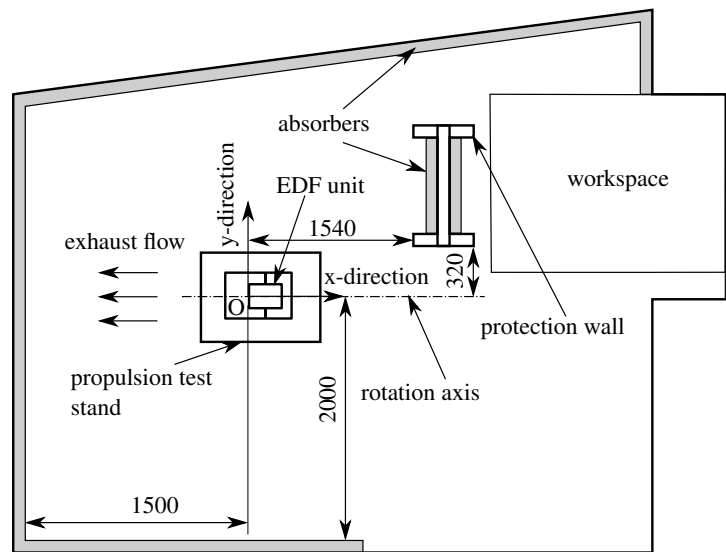


Figure 3: Setup and dimensions of the measuring room and positioning of the propulsion test stand inside the measuring room, adapted from [3].

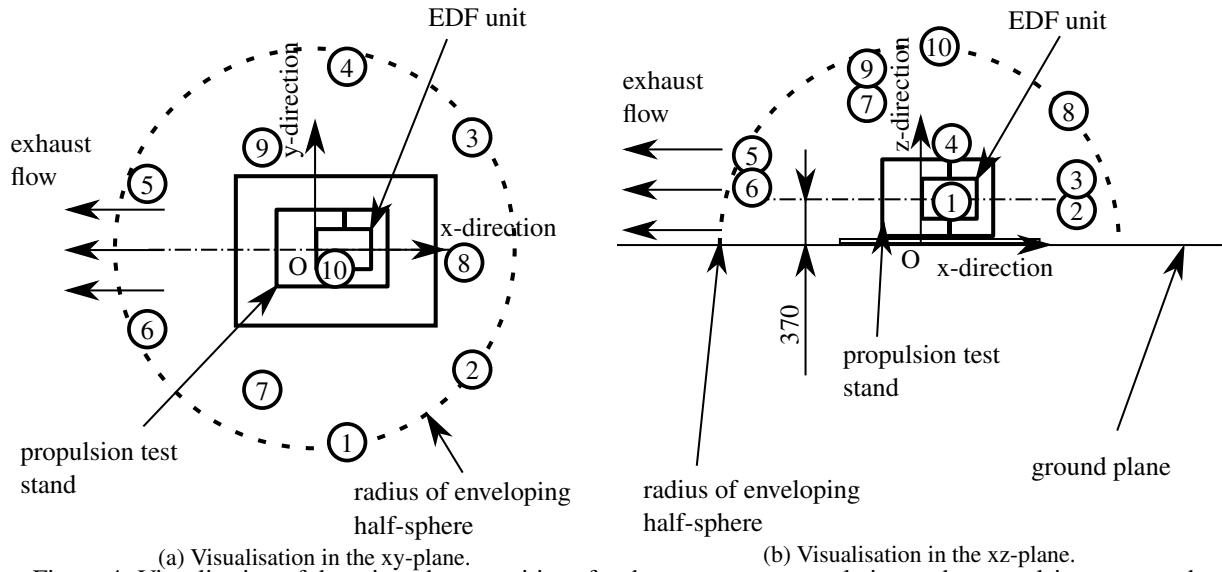


Figure 4: Visualisation of the microphone positions for the measurements relative to the propulsion test stand.

according to the international standard DIN EN ISO 3744:2011-02 [11], 10 microphones were positioned on an enveloping surface in the form of a half-sphere in the configuration proposed for measuring arbitrary sound sources in [11] (see Figure 4). The EDF unit was positioned in the measuring room as presented in Figure 3 to minimize the effects of surrounding walls on the EDF unit's flow field. However, free flow conditions could not be achieved, as the exhaust flow meets the rear wall of the measuring room at a distance of 1.5 m. No avoiding measures to reduce the impinging jet on the room walls were used during the experiments. The measurement campaign produced reliable results since the overall goal was to understand the noise mechanisms and a possible mitigation strategy by comparing two manufactured variants. The sampling rate for the measurements was $f_s = 48$ kHz, the measuring time at each operating point was 20 s and the acoustic sensors that were used for the measurements were pre-polarised back-electret condenser microphones with wind-screens.

The measurement results were corrected with the measuring room's reverberation characteristics and the individual microphones' frequency-dependent sensitivities. The measuring range is limited to frequencies above 300 Hz accounting for the acoustic properties of the measuring room [11]. Finally, the A-weighted sound power level spatially averaged across all microphone positions $\overline{L_{W,A}}$ is computed.

3 Sound Power Measurements Results

The measurements of the EDF were conducted at the four operating points and evaluated as narrowband-signals $L_{W,A}$ in Figure 5. The four highest tonal sound power levels (SWL) are at the BPF and its harmonics at all operating points. Moreover, at OP2, OP3, and OP4, the highest tonal SWL is at the BPF itself, which leads to aerodynamic effects as the primary acoustic source for the EDF unit at those operating points. For the tonal components at the BPF itself, the source mechanisms can be traced back to aerodynamic reasons. In contrast, the higher harmonic frequencies of the BPF can also be caused by the noise coming from the electric powertrain, as described above. However, at OPI, the highest tonal SWL is at the third harmonic frequency of the BPF, which also showed high SWLs in acoustic measurements of the electric powertrain only. In this OPI and at the third harmonic, the electric powertrain emissions dominate the peak. Therefore, the source mechanism can be a parasitic clogging torque characteristic of the electric motor at this operating point. Also noteworthy is that at OPI, a hump between the BPF and the first harmonic occurs.

The highest broadband SWLs are between 4 kHz to 6 kHz and increase in amplitude with increasing rotational speed. Microphone array measurements support the rotor self-noise mechanisms to be the acoustic sources of those broadband SWL [3]. Former research [12] also showed that tip noise mechanisms and boundary layer noise contribute to the broadband noise of the present measuring object. The highest narrowband components of the frequency spectrum are at 350 Hz to 450 Hz and do not change in their frequency with increasing rotational speed. One hypothesis for the noise mechanism of those narrowband components can be acoustic resonances of the electric motor cavity because those narrowband components have also been detected in subsequent measurements of the EDF's electric powertrain. Additionally, acoustic resonances of this kind have already been detected in [9].

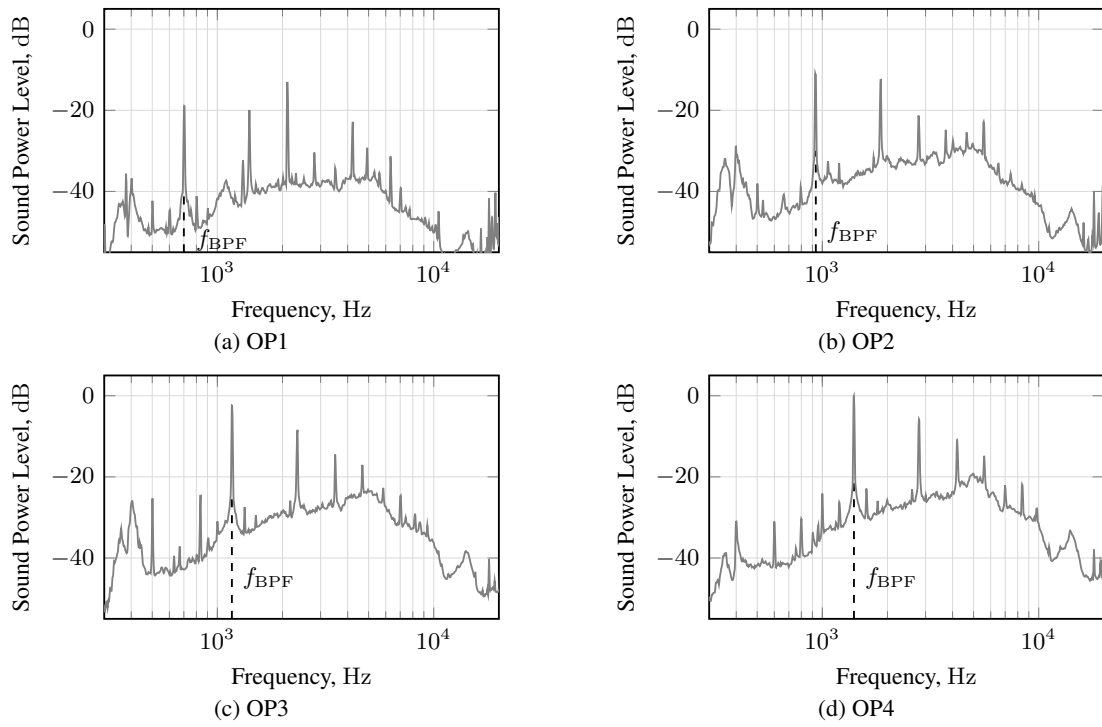


Figure 5: Narrowband $\overline{L}_{W,A}$ at different operating points relative to the highest narrowband sound power level in the observed operating range.

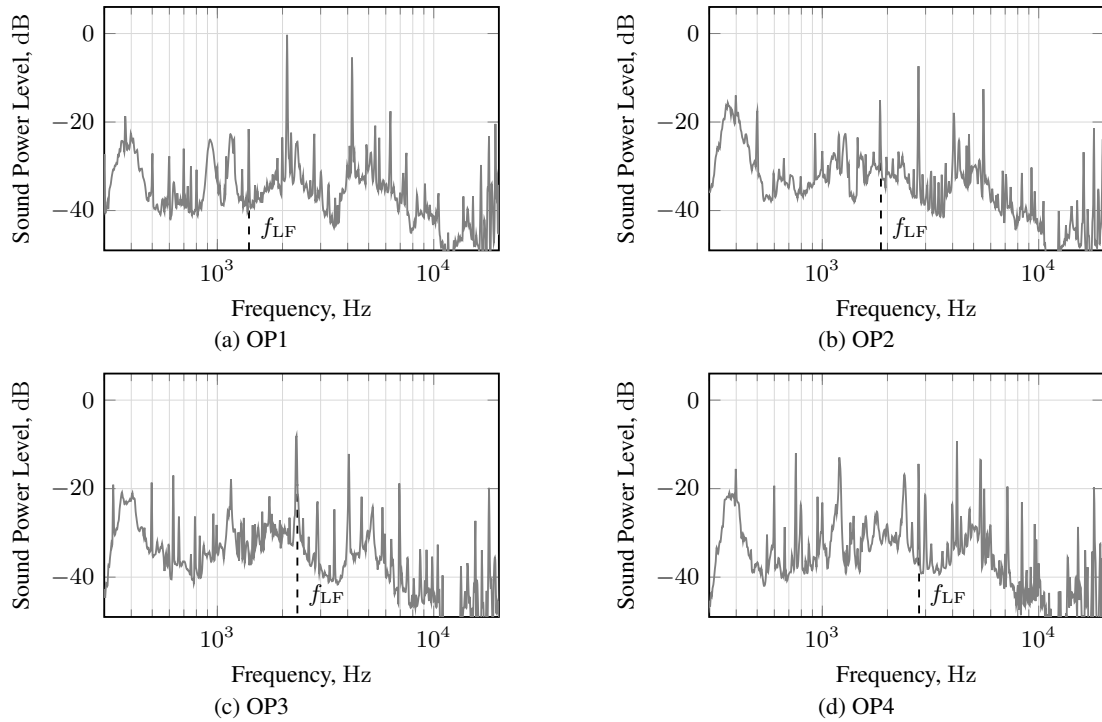


Figure 6: Narrowband $\overline{L}_{W,A}$ of the electric powertrain without load at different operating points relative to the highest narrowband sound power level in the observed operating range.

The frequency components above 15 kHz do neither vary in amplitude nor frequency with increasing rotational speed and are excited by the electronic motor controller's transistor operations. This so-called switching noise is an acoustic property of powertrains, including an ECM, because high-frequency transistor operations inside the motor controller achieve the electric phase commutation.

In a second measurement campaign, the fan was removed to detect the odd behavior of some noise emissions. Additionally, we investigate the proportion of the noise that comes from the EDF electric powertrain without having the influence of the fan. With the presented setup, it is not possible to make statements about the absolute SPL amplitudes of the ECM and the motor controller under load because the ECM's internal currents and electromagnetic forces are lowered. However, a first estimation can be made on the relevant frequency components of the acoustic spectrum. Additionally, an extrapolation or compensation based on physical considerations regarding the electric current would be possible.

In **Figure 6**, the powertrain measurement results at the four operating points are shown. The highest tonal SWL of the powertrain that was measured without load at OP1 occurs at 2100 Hz, which is the BPF's third harmonic for the EDF system. Subsequently, the primary source mechanism for this tonal noise component can be the electric powertrain in clogging torque characteristics. At all four operating points, the highest emitted tonal SWLs of the electric powertrain occurred at multiplicities of the rotational speed, which further strengthens the assumption of electromagnetic local and global forces being the main sound source mechanisms. The narrowband SWLs at 350 Hz and 400 Hz are also detected in the measurements of the electric powertrain, which excludes the aerodynamic rotor as their noise source. A possible explanation is acoustic resonances of the motor's internal airspace between its rotor and stator because these narrowband SWL are independent of the rotational speed. A similar noise mechanism has already been identified in [9].

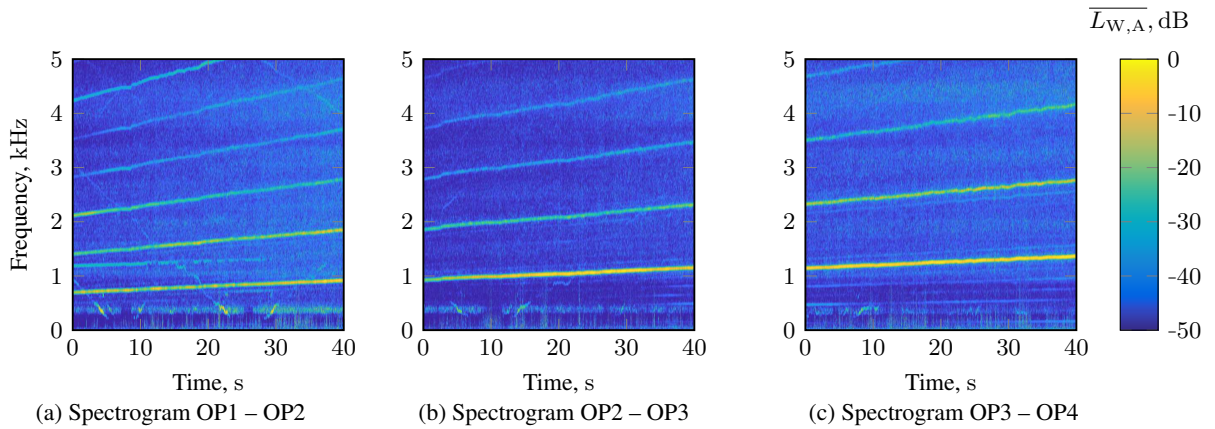


Figure 7: $\overline{L_{W,A}}$ of the EDF system between neighbouring operating points relative to the highest sound power level in the respective measurement range.

Additional measurements of the EDF system's SWL were performed in the form of transient measurements with a constant rotational speed increase. Therefore, 40 s measurements were done between the neighboring operating point using the same measuring setup as presented in **section 2**. The SWL $\overline{L_{W,A}}$ denotes the measured SWL relative to the highest SWL in the respective measurement range. Across the operating range, the BPF and its harmonics show high SWLs in the spectra, which confirms the presence of aerodynamic sources as the rotor and the rotor-stator interaction throughout the observed operating range.

In **Figure 7**, the narrowband SWL in the range between 350 Hz and 450 Hz can be confirmed to have a constant frequency band across the operating range observed. One single tonal component in **Figure 7a** obtains a constant frequency of 1200 Hz. It decays with increasing rotational speed while completely vanishing at 30 s, which can be described by an aerodynamic resonance of the EDF system.

Across the speed range from OP1 to OP3, there are repeating discontinuous artifacts that appear to be dependent on the rotational speed piecewise in a linear relation. Those artifacts can be identified in **Figure 7a** and **Figure 7b** as linearly decreasing in frequency, vanishing, and then linearly increasing in frequency with ascending rotational speed. Four of those artefacts can be distinguished across the considered operating range, with the first artefact in **Figure 7a** vanishing from 5 s to 10 s, the second artefact in **Figure 7a** vanishing between 23 s and 30 s, the third artefact in **Figure 7b** vanishing between 6 s and 13 s and the fourth artefact in **Figure 7c** vanishing between 1 s and 8 s. As the ECM was assumed to be the source for the noise mechanism for these artifacts, the electric powertrain was measured transiently without the aerodynamic rotor attached in the considered operating range.

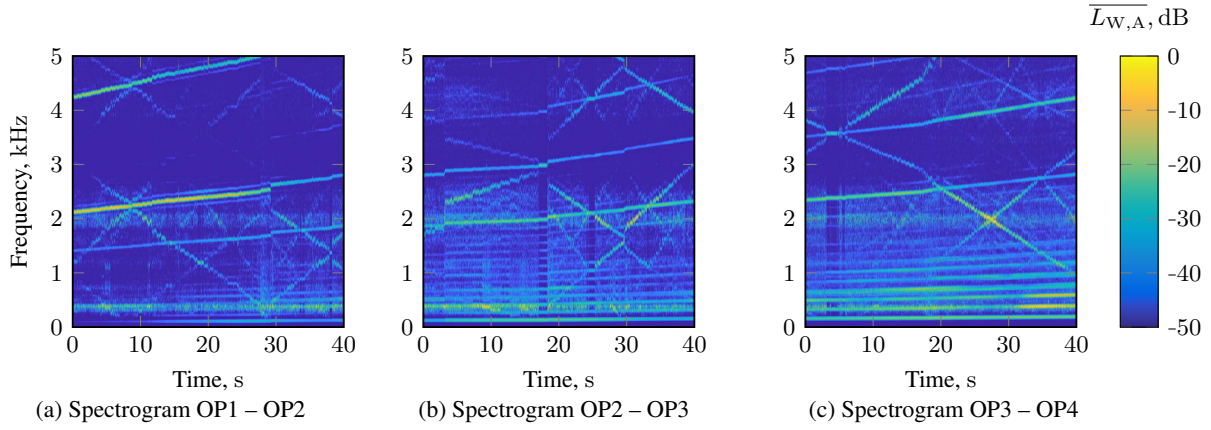


Figure 8: $\overline{L_{W,A}}$ of the electric powertrain between neighbouring operating points relative to the highest sound power level in the respective measurement range.

The exact measurements for the whole operating range were conducted for the electric powertrain's noise without the fan attached. For better visualization of the frequency component's dependence of the electric powertrain's noise on rotational speed, again, the measurement results are plotted in the form of spectrograms as formerly described for the whole operating range in Figure 8. We determined from Figure 8 that the ascend of the rotational speed was not constant across the entire operating range due to controlling difficulties of the motor controller operating the ECM without load. The tonal frequency components at the primary electromagnetic frequency f_{LF} , other electromagnetic frequencies, and their harmonics are notably visible. The artifact forms that first decrease their frequency with increasing rotational speed are also seen in the measurement results from the electric powertrain. Accordingly, the respective source mechanism can be assigned to the electric drive. One explanation can be a commutation operating principle of the inverter, but a closer examination of the electronic components needs to be conducted to prove this hypothesis.

4 Effects of Acoustic Liner

Regarding the previous measurement campaigns, the design of the EDF unit was modified by the placement of acoustic liners inside the duct. These liners were used to reduce the emitted sound power in the operating range overall. Based on the two variants, the A-weighted overall sound power level (OSPL) was measured, computed, and compared for the two variants (see Figure 9). Without optimizing the position and the design concerning the noise mitigation, the placement of the acoustic liners decreased the emitted noise over a broad operating range.

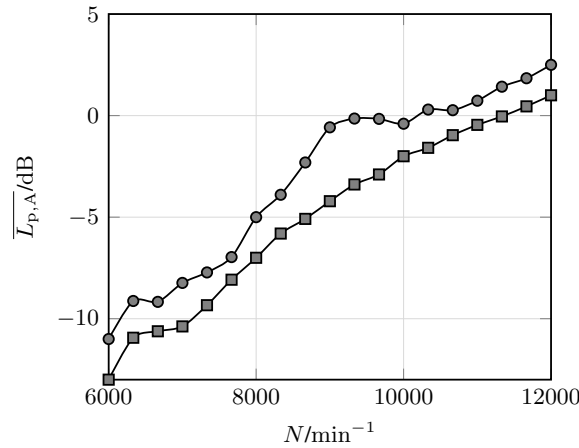


Figure 9: A-weighted OSPL over operating range of unmodified (●) and modified (■) EDF unit.

5 Conclusion and Suggestions

The acoustic examination of the EDF unit in the observed operating range has shown expected tonal components at the BPF and its harmonic frequencies. The acoustic components with the highest measured sound power levels were traced to aerodynamic reasons. In contrast, some frequency components with minor sound power levels could be assigned to the electric powertrain components. The base frequency of the ECM's electromagnetic local forces was found to be a main tonal frequency component of the electric powertrain's emitted noise in measurements without the EDF's aerodynamic components' noise sources. Artifacts with discontinuous dependence on the rotational speed were found in spectrograms of transient measurements of the electric powertrain, therefore assigned to the electric powertrain as the noise source. The influence of the electric powertrain on the acoustic characteristics of the EDF is shown to be significant. Regarding the measurement results of the electric powertrain in contrast to the entire EDF unit, an extrapolation or compensation based on physical considerations regarding the electric current would be interesting to make the results comparable. Furthermore, a next measurement campaign will adjust the test rig to analyze the effects of the electric powertrain profoundly. It has to be verified and examined closer with electric measurements of the single motor phases in the operating range. Through the findings of this work, the acoustic emissions of the EDF can be better understood and further improved.

References

- [1] Pascioni, K., and Rizzi, S. A., "Tonal Noise Prediction of a Distributed Propulsion Unmanned Aerial Vehicle," *2018 AIAA/CEAS Aeroacoustics Conference*, 2018, p. 2951.
- [2] Kim, H. D., Perry, A. T., and Ansell, P. J., "A review of distributed electric propulsion concepts for air vehicle technology," *2018 AIAA/IEEE Electric Aircraft Technologies Symposium (EATS)*, IEEE, 2018, pp. 1–21.
- [3] Schmidt, J., and Schoder, S., *Acoustic Optimisation of an Electric Ducted Fan Unit through Absorber Design and Placement*, Vienna University of Technology, 2020.
- [4] Smith, M. J., *Aircraft noise*, Vol. 3, Cambridge University Press, 2004.
- [5] Tyler, J. M., and Sofrin, T. G., "Axial flow compressor noise studies," Tech. rep., SAE Technical Paper, 1962.
- [6] Griffiths, J., "The spectrum of compressor noise of a jet engine," *Journal of Sound and Vibration*, Vol. 1, No. 2, 1964, pp. 127–140.
- [7] Gieras, J. F., Wang, C., and Lai, J. C., *Noise of polyphase electric motors*, CRC press, 2018.
- [8] Ko, H.-S., and Kim, K.-J., "Characterization of noise and vibration sources in interior permanent-magnet brushless DC motors," *IEEE Transactions on Magnetics*, Vol. 40, No. 6, 2004, pp. 3482–3489.
- [9] Lee, H. J., Chung, S. U., and Hwang, S. M., "Noise source identification of a BLDC motor," *Journal of mechanical science and technology*, Vol. 22, No. 4, 2008, p. 708.
- [10] Pindoriya, R., Mishra, A., Rajpurohit, B., and Kumar, R., "An analysis of vibration and acoustic noise of BLDC motor drive," *2018 IEEE Power & Energy Society General Meeting (PESGM)*, IEEE, 2018, pp. 1–5.
- [11] e.V., D., *3744: 2011-02: Akustik – Bestimmung der Schallleistungs- und Schallenergiepegel von Geräuschquellen aus Schalldruckmessungen – Hüllflächenverfahren der Genauigkeitsklasse 2 für ein im Wesentlichen freies Schallfeld über einer reflektierenden Ebene (ISO 3744: 2010)*, Beuth-Verlag, Berlin, 2011.
- [12] Krömer, F. J., "Sound emission of low-pressure axial fans under distorted inflow conditions," Doctoral thesis, FAU University Press, 2018. <https://doi.org/10.25593/978-3-96147-089-1>.
- [13] Floss, S., *Mitigation of sound by micro-perforated absorbers in different types of sound fields - design and evaluation*, Vienna University of Technology, 2022.